Structural Engineering and Mechanics, *Vol. 65, No. 5 (2018) 523-533*
DOI: https://doi.org/10.12989/sem.2018.65.5.523

Dynamic response of functionally graded annular/circular plate in contact with bounded fluid under harmonic load

Sh. Yousefzadeh[1a], A. A. Jafari*[2], A. Mohammadzadeh[1b] and M. Najafi[1c]

[1]*Department of Mechanical and Aerospace Engineering, Science and Research Branch, Islamic Azad University, Tehran, Iran*
[2]*Department of Mechanical Engineering, K. N. Toosi University of Technology, Tehran, Iran*

(Received March 19, 2017, Revised December 12, 2017, Accepted January 4, 2018)

Abstract. In this study, the dynamic response of a functionally graded material (FGM) circular plate in contact with incompressible fluid under the harmonic load is investigated. Analysis of the plate is based on First-order Shear Deformation Plate Theory (FSDT). The governing equation of the oscillatory behavior of the fluid is obtained by solving Laplace equation and satisfying its boundary conditions. A new set of admissible functions, which satisfy both geometrical and natural boundary conditions, are developed for the free vibration analysis of moderately thick circular plate. The Chebyshev-Ritz Method is employed together with this set of admissible functions to determine the vibrational behaviors. The modal superposition approach is used to determine the dynamic response of the plate exposed to harmonic loading. Numerical results of the force vibrations and the effects of the different geometrical parameters on the dynamic response of the plate are investigated. Finally, the results of this research in the limit case are compared and validated with the results of other researches and finite element model (FEM).

Keywords: dynamic response; circular plate; chebyshev-ritz method; functionally graded material; first order shear deformation plate theory

1. Introduction

Vibration of structures in contact with fluids is a coupled fluid-elastic phenomenon. Hydroelastic characteristics of plates in contact with fluid are important in various engineering applications such as nuclear engineering, aerospace structures, liquid storage tanks, reactor internal components, solar plates and offshore naval or marine structures. Fluid-coupled vibrations may be caused to the structural fatigue and failure (Shafiee 2014, Amiri 2013). Thus, a good understanding of the dynamic interactions between an elastic plate and fluid is necessary (Hasheminejad 2013). It is well established that the natural frequencies of structures in contact with fluid are different from those in air (Kerboua 2008). Several researchers have focused their attention on investigating the dynamics of the structures and their behavior in contact with fluid. Kwak and Kim (1991) concerned the effect of fluid on the natural frequencies of circular plates vibrating axisymmetric. They obtained the non-dimensional added mass incremental factor for circular plates with various boundary conditions. Hossini- Hashemi *et al.* (2010) studied free vibration of FGM rectangular plate using first order shear deformation plate theory. They presented analytical solution for vibration of FGM plate on Winkler elastic foundation. Allahverdizadeh *et al.* (2008) developed a semi-analytical approach for nonlinear free and forced axisymmetric vibration of thin circular functionally graded plate. They solved the governing equations of the plate by using assumed-time-mode and Kantorovich method for harmonic vibrations. Haddara and Cao (1996) investigated the dynamic response of flat horizontal plates vibrating in air and under water. They studied the effects of the boundary conditions and the depth of the submergence of the plate on the natural frequencies. Tariverdilo *et al.* (2013) considered the free vibration of an asymmetric clamped circular plate in contact with incompressible fluid and obtained the natural frequencies and relevant added mass for their problem. They used two approaches to derive the free vibration frequencies of the system. Jeong (2003) dealt with the free vibration of two identical circular plates coupled with a bounded fluid. He suggested an analytical method based on the finite Fourier-Bessel expansion and Rayleigh-Ritz method. In their work, the effect of gap between the plates on the fluid-coupled natural frequencies is investigated. Khorshidi and Bakhsheshi (2014) analyzed the natural frequencies of a vertical FGM composite rectangular plate in contact with fluid on its faces. They calculated the natural frequencies of the plate coupled with sloshing fluid modes using Rayleigh-Ritz method and based on minimizing the Rayleigh quotient. Dong (2008) investigated three dimensional free vibrations of functionally graded annular plates with different boundary conditions using Chebyshev-Ritz method. Kwak (1997)

*Corresponding author, Professor
E-mail: ajafari@kntu.ac.ir
[a]Ph.D. Student
E-mail: sh.yoosefzadeh@gmail.com
[b]Ph.D.
E-mail: a-mohamadzadeh@srbiau.ac.ir
[c]Ph.D
E-mail: najafi@srbiau.ac.ir

ISSN: 1225-4568 (Print), 1598-6217 (Online)

analyzed the virtual mass effect due to the presence of water on the natural frequencies of circular plates. He obtained the non-dimensional added virtual mass incremental factors by employing the integral transformation technique in conjunction with the Fourier-Bessel series approach. More recently, Jeong *et al.* (2009) developed a theoretical Reyleih-Ritz to estimate the coupled natural frequencies of a vertical clamped circular plate partially in contact with an ideal incompressible liquid.

Cho *et al.* (2015) developed the numerical procedure for the forced vibration analysis of bottom and vertical rectangular plate structures in contact with fluid, subjected to internal point harmonic excitation force. Lagrange's equation of motion was utilized to formulate the eigenvalue problem taking into account potential and kinetic energies of a plate and reinforcements, and fluid kinetic energy which was calculated according to potential flow theory, respectively. Civalek (2008) investigated the effects of some geometric parameters and density variation on frequency characteristics of the circular and annular plates with varying density. The discrete singular convolution method based on regularized Shannon's delta kernel was applied to obtain the frequency parameter. The obtained results were compared with the analytical and numerical results of other researchers, which showed well agreement.

Bedroud *et al.* (2016) studied the buckling analysis of FGM circular/annular nano-plates under uniform in-plane radial compressive load with a concentric internal ring support and elastically restrained edges using an exact analytical approach within the framework of nonlocal Mindlin plate theory. Their study showed that an internal ring support can increase the buckling capacity, accordingly this capacity is maximized when the internal ring support is located at an optimal position. Akgoz and Civalek (2013) investigated the buckling problem of linearly tapered micro-columns on the basis of modified strain gradient elasticity theory. They used Bernoulli-Euler beam theory to model the non-uniform micro column. Rayleigh-Ritz solution method was utilized to obtain the critical buckling loads of the tapered cantilever micro-columns for different taper ratios. Their study showed that the differences between critical buckling loads achieved by classical and those predicted by non-classical theories are considerable.

Levy (1996) concerned with the structural optimization problem of maximizing the compressive buckling load of orthotropic rectangular plates for a given volume of material. His study stated that the thickness distribution is proportional to the strain energy density contrary to popular claims of constant strain energy density at the optimum. A double cosine thickness varying plate and a double sine thickness varying plate were then fine-tuned in a one parameter optimization using the Rayleigh-Ritz method of analysis. Tahouneh (2014) dealt with the free vibration analysis of bidirectional functionally graded annular plates resting on a two-parameter elastic foundation. The formulations were based on the three-dimensional elasticity theory. He presented a novel 2-D six-parameter power-law distribution for ceramic volume fraction of 2-D functionally graded materials that gives designers a powerful tool for flexible designing of structures under multi-functional requirements. The interesting results indicated that a graded ceramic volume fraction in two directions has a higher capability to reduce the natural frequency than conventional 1-D functionally graded materials.

Jhung *et al.* (2005) investigated the free vibration of a circular plate in contact with a fluid; submerged in fluid, beneath fluid or on fluid. An analytical method based on the finite Fourier-Bessel series expansion and Rayleigh-Ritz method was suggested. The proposed method was verified by the finite element analysis using commercial program with a good accuracy. They obtained the normalized natural frequencies in order to estimate the relative added mass effect of fluid on each vibration mode of the plate. Civalek (2004) presented a comparison between the methods of differential quadrature (DQ) and harmonic differential quadrature (HDQ) for buckling, bending, and free vibration analysis of thin isotropic plates and columns. He showed that the HDQ method gives more accurate results and needs less grid points than the DQ method. Civalek *et al.* (2010) presented the buckling analysis of rectangular plates subjected to various in-plane compressive loads using Kirchhoff plate theory. They adopted the method of discrete singular convolution. Linearly varying, uniform and non-uniform distributed load conditions were considered on two-opposite edges for buckling. The results were obtained for different types of boundary conditions and aspect ratios. Functionally graded materials (FGM) have appeal properties of high strength, minimum weight and ultra-high temperature resistance and were first introduced by a group of Japanese scientists. A typical FGM is an inhomogeneous composite made of different phases of material constituents usually metal and ceramic with a high bending-stretching coupling effect was reported by Shen. By gradually varying the volume fraction of constituent materials, the material properties of functionally graded materials vary smoothly and change continuously between different layers. This advantage eliminates interface problems of composite materials and the stress distribution becomes smooth (Shen 2016).

The above review clearly indicates that while there exist a notable body of literature on the free vibrational characteristics of fluid-coupled with homogeneous plates, little has been done on theoretical or numerical solutions of fluids in contact with FGM plates. This paper presents a theoretical method to calculate the dynamic response of a circular FGM plate partially contacting with bounded fluid, and subject to harmonic load, using Reyleih-Ritz method. In the developed model, the first order shear deformation theory is used to obtain the kinetic and strain energies of the plate. Transverse displacement of the plate is, thereafter, approximated by a set of admissible trial functions which satisfy the boundary conditions. The equations governing the oscillatory behavior of the fluid are obtained by solving Laplace equation and satisfying its pertinent boundary conditions. The proposed analytical method is verified by comparing it with similar published works. Finally, the influences of the boundary conditions, plate and vessel dimensions, fluid density and depth on the plate displacements are discussed in details.

2. Formulation

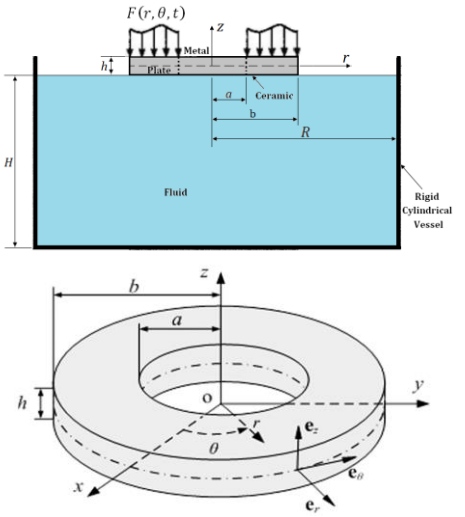

Fig. 1 Circular plate in contact with fluid with coordinate convection

2.1 Formulation for free vibration of circular plate

Fig. 1 depicts a FGM circular plate under excited force $F(r,\theta,t)$, partially in contact with fluid in a rigid cylindrical vessel. a, b and h represent the internal radius, external radius and thickness of the circular plate respectively. R and H refer to radius and depth of the vessel respectively.

According to Mindlin's plate theory, in polar coordinate, the displacement components are given by (Jomehzadeh 2009)

$$\begin{aligned} u_1 &= u_r + z\psi_r \\ u_2 &= u_\theta + z\psi_\theta \\ u_3 &= u_z \end{aligned} \tag{1}$$

Where z is the thickness coordinate, u_1, u_2 and u_3 are the displacements along the r, θ and z axes respectively. u_r and u_θ are the displacement of mid-plane along the r and θ directions respectively. ψ_r and ψ_θ are the rotational displacements about the r and θ axes respectively. Under the assumption of small deformation and linear strain-displacement relationships, the strain components of FGM circular plate can be expressed as

$$\begin{aligned} \varepsilon_{rr} &= \frac{\partial u_1}{\partial r} = \left(\frac{\partial u_r}{\partial r} + z\frac{\partial \psi_r}{\partial r}\right), \\ \varepsilon_{\theta\theta} &= \frac{1}{r}\left(u_1 + \frac{\partial u_2}{\partial \theta}\right) = \frac{1}{r}\left(u_r + \frac{\partial u_\theta}{\partial \theta}\right) + \frac{z}{r}\left(\psi_r + \frac{\partial \psi_\theta}{\partial \theta}\right), \\ 2\varepsilon_{r\theta} &= \frac{1}{r}\frac{\partial u_1}{\partial \theta} + \frac{\partial u_2}{\partial r} - \frac{u_2}{r} \\ &= \left(\frac{1}{r}\frac{\partial u_r}{\partial \theta} + \frac{\partial u_\theta}{\partial r} - \frac{u_\theta}{r}\right) \\ &\quad + z\left(\frac{1}{r}\frac{\partial \psi_r}{\partial \theta} + \frac{\partial \psi_\theta}{\partial r} - \frac{\psi_\theta}{r}\right), \end{aligned} \tag{2}$$

$$\begin{aligned} 2\varepsilon_{rz} &= \left(\frac{\partial u_1}{\partial z} + \frac{\partial u_3}{\partial r}\right) = \left(\psi_r + \frac{\partial u_z}{\partial r}\right), \\ 2\varepsilon_{\theta z} &= \left(\frac{\partial u_2}{\partial z} + \frac{1}{r}\frac{\partial u_3}{\partial \theta}\right) = \left(\psi_\theta + \frac{1}{r}\frac{\partial u_z}{\partial \theta}\right), \end{aligned}$$

Considering plane stress state for FGM plate, the stresses are evaluated as

$$\begin{aligned} \sigma_{rr} &= \frac{E(z)}{1-\nu^2}(\varepsilon_{rr} + \nu\varepsilon_{\theta\theta}), \\ \sigma_{\theta\theta} &= \frac{E(z)}{1-\nu^2}(\varepsilon_{\theta\theta} + \nu\varepsilon_{rr}), \\ \sigma_{r\theta} &= \frac{E(z)}{2(1+\nu)}(2\varepsilon_{r\theta}), \\ \sigma_{\theta z} &= \frac{E(z)}{2(1+\nu)}(2\varepsilon_{\theta z}), \\ \sigma_{rz} &= \frac{E(z)}{2(1+\nu)}(2\varepsilon_{rz}) \end{aligned} \tag{3}$$

Where ν is Poisson's ratio, considered to be constant throughout the volume of the plate. $E(z)$ is the variable Young's modulus of the plate in the $z-$direction, evaluated as following (Mehrabadi 2009)

$$E(z) = E_m + (E_c - E_m)\left(\frac{1}{2} - \frac{z}{h}\right)^p \tag{4}$$

In which E_m and E_c are modulus of elasticity of metal and ceramic respectively and p is the volume fraction index which assume values greater than or equal to zero. For the value of $p = 0$, a fully ceramic plate is intended.

Introducing the following dimensionless parameters (Dong 2008)

$$\bar{r} = \frac{2r}{\bar{R}} - \delta, \qquad \bar{\theta} = \theta, \qquad \bar{z} = \frac{2z}{h}, \qquad \eta = \frac{a}{b}, \qquad \lambda = \frac{h}{b} \tag{5}$$

Where $\bar{R} = b - a$ and $\delta = (b+a)/(b-a)$.

Free vibration displacements of the plate are expressed as (Jafari 2008, Khdeir 1988)

$$\begin{aligned} u_r(\bar{r},\bar{\theta},t) &= \bar{U}_r(\bar{r})\cos n\bar{\theta}\, e^{i\omega t} \\ &= F_1^a(\bar{r})F_1^b(\bar{r})\sum_{i=1}^{I} u_{ri}R_i(\bar{r})\cos n\bar{\theta}\, e^{i\omega t} \\ u_\theta(\bar{r},\bar{\theta},t) &= \bar{U}_\theta(\bar{r})\sin n\bar{\theta}\, e^{i\omega t} \\ &= F_2^a(\bar{r})F_2^b(\bar{r})\sum_{j=1}^{J} u_{\theta j}R_j(\bar{r})\sin n\bar{\theta}\, e^{i\omega t} \end{aligned} \tag{6}$$

$$u_z(\bar{r},\bar{\theta},t) = \bar{U}_z(\bar{r})\cos n\bar{\theta}\, e^{i\omega t} \tag{7}$$

$$= F_3^a(\bar{r})F_3^b(\bar{r})\sum_{k=1}^{K} u_{zk}R_k(\bar{r})\cos n\bar{\theta}\, e^{i\omega t} \tag{8}$$

$$\psi_r(\bar{r},\bar{\theta},t) = \bar{\psi}_r\cos n\bar{\theta}\, e^{i\omega t} \tag{9}$$

$$= F_r^a(\bar{r})F_r^b(\bar{r})\sum_{l=1}^{L} \psi_{rl}R_l(\bar{r})\cos n\bar{\theta}\, e^{i\omega t} \tag{10}$$

$$\begin{aligned} \psi_\theta(\bar{r},\bar{\theta},t) &= \bar{\psi}_\theta\sin n\bar{\theta}\, e^{i\omega t} \\ &= F_\theta^a(\bar{r})F_\theta^b(\bar{r})\sum_{q=1}^{Q} \psi_{\theta q}R_q(\bar{r})\sin n\bar{\theta}\, e^{i\omega t} \end{aligned}$$

In which I, J, K, L and Q truncation orders of the Chebyshev polynomial series and u_{ri}, $u_{\theta j}$, u_{zk}, ψ_{rl} and $\psi_{\theta q}$ are unknown coefficients to be determined and $R_f(\bar{r})$ $(f = i, j, k, l, q)$ is the one-dimensional fth Chebyshev polynomial that defined as

Table 1 Mechanical boundary functions for different boundary conditions

Boundary conditions	Boundary functions									
	Inner edge					Outer edge				
	$F_1^a(\bar{r})$	$F_2^a(\bar{r})$	$F_3^a(\bar{r})$	$F_r^a(\bar{r})$	$F_\theta^a(\bar{r})$	$F_1^b(\bar{r})$	$F_2^b(\bar{r})$	$F_3^b(\bar{r})$	$F_r^b(\bar{r})$	$F_\theta^b(\bar{r})$
F-F	1	1	1	1	1	1	1	1	1	1
C-C	$1+\bar{r}$	$1+\bar{r}$	$1+\bar{r}$	$1+\bar{r}$	$1+\bar{r}$	$1-\bar{r}$	$1-\bar{r}$	$1-\bar{r}$	$1-\bar{r}$	$1-\bar{r}$
F-C	1	1	1	1	1	$1-\bar{r}$	$1-\bar{r}$	$1-\bar{r}$	$1-\bar{r}$	$1-\bar{r}$
C-F	$1+\bar{r}$	$1+\bar{r}$	$1+\bar{r}$	$1+\bar{r}$	$1+\bar{r}$	1	1	1	1	1

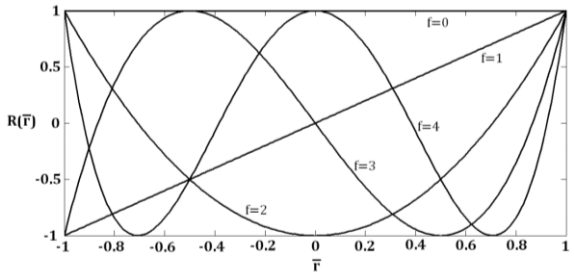

Fig. 2 The first five terms of the Chebyshev polynomials

$$R_f(\bar{r}) = \cos(f\cos^{-1}\bar{r}) \qquad \bar{r}\in[-1,1]\ , \quad f = 0,1,2,\ldots \tag{11}$$

$F_e^a(\bar{r})$ and $F_e^b(\bar{r})$ $(e = 1,2,3,r,\theta)$ are boundary functions satisfying the inner and outer geometric boundary conditions. The boundary functions corresponding to classical boundary conditions are given in Table 1 (Zhou 2003).

It should be noted that Chebyshev series is a set of complete and orthogonal series in the interval [-1, 1]. Chebyshev polynomials are well known to provide an excellent and rapid convergence and better stability in approximate solutions than other polynomials (Fox 1968). The first five Chebyshev polynomials are given in Fig. 2.

Introducing Eqs. (6)-(10) into the strain components (2) gives

$$\begin{aligned}
\varepsilon_{rr} &= \frac{2}{\bar{R}}\left(\frac{\partial\bar{U}_r}{\partial\bar{r}} + \bar{z}\frac{h}{2}\frac{\partial\bar{\psi}_r}{\partial\bar{r}}\right)\cos n\bar{\theta}\, e^{i\omega t},\\
\varepsilon_{\theta\theta} &= \frac{2}{\bar{R}(\bar{r}+\delta)}\left[(\bar{U}_r + n\bar{U}_\theta) + \bar{z}\frac{h}{2}(\bar{\psi}_r + n\bar{\psi}_\theta)\right]\cos n\bar{\theta}\, e^{i\omega t},\\
2\varepsilon_{r\theta} &= \left(-\frac{2}{\bar{R}(\bar{r}+\delta)}(n\bar{U}_r + \bar{U}_\theta) + \frac{2}{\bar{R}}\frac{\partial\bar{U}_\theta}{\partial\bar{r}}\right) + \bar{z}\frac{h}{2}\left(-\frac{2}{\bar{R}(\bar{r}+\delta)}(n\bar{\psi}_r + s\bar{\psi}_\theta) + \frac{2}{\bar{R}}\frac{\partial\bar{\psi}_\theta}{\partial\bar{r}}\right)\sin n\bar{\theta}\, e^{i\omega t},\\
2\varepsilon_{rz} &= \left(\bar{\psi}_r + \frac{2}{\bar{R}}\frac{\partial\bar{U}_z}{\partial\bar{r}}\right)\cos n\bar{\theta}\, e^{i\omega t}\\
2\varepsilon_{\theta z} &= \left(\bar{\psi}_\theta - \frac{2n}{\bar{R}(\bar{r}+\delta)}\bar{U}_z\right)\sin n\bar{\theta}\, e^{i\omega t},
\end{aligned} \tag{12}$$

Substituting strain components in Eq. (12) into Eq. (3) yields

$$\begin{aligned}
\sigma_{rr} &= \frac{E(z)}{1-\nu^2}\left[\frac{2}{\bar{R}}\left(\frac{\partial\bar{U}_r}{\partial\bar{r}} + \bar{z}\frac{h}{2}\frac{\partial\bar{\psi}_r}{\partial\bar{r}}\right) + \frac{2\nu}{\bar{R}(\bar{r}+\delta)}\left[(\bar{U}_r + n\bar{U}_\theta) + \bar{z}\frac{h}{2}(\bar{\psi}_r + n\bar{\psi}_\theta)\right]\right]\cos n\bar{\theta}\, e^{i\omega t},\\
\sigma_{\theta\theta} &= \frac{E(z)}{1-\nu^2}\left[\frac{2}{\bar{R}(\bar{r}+\delta)}\left[(\bar{U}_r + n\bar{U}_\theta) + \bar{z}\frac{h}{2}(\bar{\psi}_r + n\bar{\psi}_\theta)\right] + \frac{2\nu}{\bar{R}}\left(\frac{\partial\bar{U}_r}{\partial\bar{r}} + \bar{z}\frac{h}{2}\frac{\partial\bar{\psi}_r}{\partial\bar{r}}\right)\right]\cos n\bar{\theta}\, e^{i\omega t},\\
\sigma_{r\theta} &= \frac{E(z)}{2(1+\nu)}\left[\left(-\frac{2}{\bar{R}(\bar{r}+\delta)}(n\bar{U}_r + \bar{U}_\theta) + \frac{2}{\bar{R}}\frac{\partial\bar{U}_\theta}{\partial\bar{r}}\right) + \bar{z}\frac{h}{2}\left(-\frac{2}{\bar{R}(\bar{r}+\delta)}(n\bar{\psi}_r + s\bar{\psi}_\theta) + \frac{2}{\bar{R}}\frac{\partial\bar{\psi}_\theta}{\partial\bar{r}}\right)\right]\sin n\bar{\theta}\, e^{i\omega t},\\
\sigma_{\theta z} &= \frac{E(z)}{2(1+\nu)}\left(\bar{\psi}_r + \frac{2}{\bar{R}}\frac{\partial\bar{U}_z}{\partial\bar{r}}\right)\cos n\bar{\theta}\, e^{i\omega t},\\
\sigma_{rz} &= \frac{E(z)}{2(1+\nu)}\left(\bar{\psi}_\theta - \frac{2n}{\bar{R}(\bar{r}+\delta)}\bar{U}_z\right)\sin n\bar{\theta}\, e^{i\omega t}
\end{aligned} \tag{13}$$

The elastic strain energy U_p of the plate is given by (Hejripour 2012)

$$U_p = \frac{1}{2}\int_{-\frac{h}{2}}^{\frac{h}{2}}\int_0^{2\pi}\int_a^b (\sigma_{ij}\varepsilon_{ij})\,r\,dr\,d\theta\,dz \qquad i,j = r,\theta,z \tag{14}$$

The elastic strain U_p in terms of dimensionless parameters (5) is expressed as

$$U_p = \frac{1}{2}\int_{-1}^{1}\int_0^{2\pi}\int_{-1}^{1}(\sigma_{ij}\varepsilon_{ij})\left(\frac{\bar{R}}{2}\right)^2\left(\frac{h}{2}\right)(\bar{r}+\delta)\,\bar{r}\,d\bar{r}\,d\bar{\theta}\,d\bar{z} \qquad i,j = r,\theta,z \tag{15}$$

The kinetic energy T_p of the plate is defined as (Hejripour 2012)

$$T_p = \frac{1}{2}\int_{-\frac{h}{2}}^{\frac{h}{2}}\int_0^{2\pi}\int_a^b \rho(z)\left[\dot{u}_1{}^2 + \dot{u}_2{}^2 + \dot{u}_3{}^2\right]r\,dr\,d\theta\,dz \qquad i,j = r,\theta,z \tag{16}$$

Eq. (16) in terms of dimensionless parameters is expressed as

$$T_p = \frac{1}{2}\int_{-1}^{1}\int_0^{2\pi}\int_{-1}^{1}\rho(z)\left[\dot{u}_1{}^2 + \dot{u}_2{}^2 + \dot{u}_3{}^2\right]\left(\frac{\bar{R}}{2}\right)^2\left(\frac{h}{2}\right)(\bar{r}+\delta)\,\bar{r}\,d\bar{r}\,d\bar{\theta}\,d\bar{z} \tag{17}$$

Where $\rho(z)$ is the mass density of the plate and is according to the volume fraction of the constitute material based on a power law function as (Mehrabadai 2009)

$$\rho(z) = \rho_m + (\rho_c - \rho_m)\left(\frac{1}{2} - \frac{z}{h}\right)^p \tag{18}$$

2.2 Formulation for fluid motion

Fig. 1 depicts a rigid and vertical vessel, partially filled with an inviscid and incompressible fluid. Potential function $\Phi(r,\theta,z,t)$ is used to describe the oscillatory fluid motion in the vessel. The fluid motion due to the plate vibration is described by the spatial velocity potential that satisfies the Laplace equation as follow (Myung 2003)

$$\nabla^2\Phi(r,\theta,z,t) = \frac{\partial^2\Phi}{\partial r^2} + \frac{1}{r}\frac{\partial\Phi}{\partial r} + \frac{1}{r^2}\frac{\partial^2\Phi}{\partial\theta^2} + \frac{\partial^2\Phi}{\partial z^2} + \frac{\partial^2\Phi}{\partial t^2} = 0 \tag{19}$$

Where $\Phi(r,\theta,z,t)$ define the velocity potential of the fluid. At the wall and the bottom of the vessel, the velocity of fluid is zero

$$\left(\frac{\partial\Phi}{\partial r}\right)_{r=R} = 0. \tag{20}$$

$$\left(\frac{\partial\Phi}{\partial z}\right)_{z=-\frac{h}{2}-H} = 0. \tag{21}$$

Employing separation of variables, the velocity potential functions $\Phi(r,\theta,z,t)$ can be written as $\Phi(r,\theta,z,t) = i\omega\varphi(r,\theta,z)\exp(i\omega t)$. Substituting this function into Eq. (15) and applying boundary conditions (20) and (21) generates the general solution of Eq. (19) as

$$\Phi(r,\theta,z,t) = i\omega.\cos n\theta \sum_{s=1}^{\infty} E_{ns} J_n\left(\frac{\beta_{ns} r}{R}\right)\left[\cosh\left(\frac{\beta_{ns} z}{R}\right) + \tanh\left(\frac{\beta_{ns}\left(H+\frac{h}{2}\right)}{R}\right)\sinh\left(\frac{\beta_{ns} z}{R}\right)\right] e^{i\omega t} \tag{22}$$

In Eq. (22), $J_n\left(\frac{\beta_{ns} r}{R}\right)$ is the Bessel function of the first kind. The frequency parameter for the fluid, β_{ns}, can be obtained by using the boundary condition (20) as follow

$$J_n'(\beta_{ns}) = 0 \tag{23}$$

The apostrophe (‘) of Eq. (23) indicate the derivative with respect to r. The positive coefficient β_{ns} can be determined by Eq. (23) for every n and s.

2.3 Interaction between the plate and fluid

The dynamic displacement of the fluid normal to the plate must coincide with that of the plate to satisfy the continuity requirement. This condition implies a permanent contact between the plate surface and the peripheral fluid layer. Hence, compatibility condition between plate and the fluid becomes

$$\left(\frac{\partial\Phi}{\partial z}\right)_{z=-\frac{h}{2}} = \frac{\partial u_z}{\partial t} \tag{24}$$

Substituting Eqs. (8) and (22) into Eq. (24), the following expression yields

$$\sum_{n=1}^{\infty}\sum_{s=1}^{\infty} E_{ns} J_n\left(\frac{\beta_{ns} r}{R}\right)\left(\frac{\beta_{ns}}{R}\right)\left[\sinh\left(\frac{\beta_{ns}\left(\frac{h}{2}\right)}{R}\right) + \tanh\left(\frac{\beta_{ns}\left(H+\frac{h}{2}\right)}{R}\right)\cosh\left(\frac{\beta_{ns}\left(\frac{h}{2}\right)}{R}\right)\right]\cos n\theta = \sum_{k=1}^{K} u_{3k} F_3^a(\bar{r}) F_3^b(\bar{r}) R_k(\bar{r})\cos n\theta \tag{25}$$

Using Fourier series (Bracewell 1986), coefficient E_{ns} can be calculated through fallowing relation

$$E_{ns} = \frac{\int_a^b r\left(\sum_{k=1}^{K} u_{zk} F_3^a(\bar{r}) F_3^b(\bar{r}) R_k(\bar{r})\right) J_n\left(\frac{\beta_{ns} r}{R}\right) dr}{\left(\frac{\beta_{ns}}{R}\right)\left[\sinh\left(\frac{\beta_{ns}\left(\frac{h}{2}\right)}{R}\right) + \tanh\left(\frac{\beta_{ns}\left(H+\frac{h}{2}\right)}{R}\right)\cosh\left(\frac{\beta_{ns}\left(\frac{h}{2}\right)}{R}\right)\right]\int_a^b r\, J_n^2\left(\frac{\beta_{ns} r}{R}\right) dr} \tag{26}$$

Therefore, the velocity potential of the fluid can be written in terms of unknown coefficients u_{zk} instead of the unknown coefficients E_{ns}.

Since the fluid is assumed as an ideal, incompressible and inviscid fluid and the free surface wave is also neglected when the plate is vibrating, the kinetic energy of the fluid can be expressed as follow (Hashemi 2010)

$$T_f = \frac{1}{2}\rho_f \int_0^{2\pi}\int_a^b \left[\Phi\left(\frac{\partial\Phi}{\partial z}\right)\right]_{z=-\frac{h}{2}} r dr d\theta \tag{27}$$

Where ρ_f is the fluid density and the domain of integration is the plate surface in contact with fluid. In order to calculate $\left(\frac{\partial\Phi}{\partial z}\right)$ the compatibility condition (24) is applied to arrive at

$$\left.\frac{\partial\Phi}{\partial z}\right|_{z=-\frac{h}{2}} = \frac{\partial u_3}{\partial t} = i\omega.F_3^a(\bar{r})F_3^b(\bar{r})\sum_{k=1}^{K} u_{3k} R_k(\bar{r})\cos n\theta\, e^{i\omega t} \tag{28}$$

Substituting relations (22) and (28) into (27) and integrating on the plate wet surface, one obtains

$$T_f = -\frac{1}{2}\rho_f \Gamma_1 \omega^2 \int_a^b F_3^a(\bar{r})F_3^b(\bar{r})\sum_{s=1}^{\infty} E_{ns} J_n\left(\frac{\beta_{ns} r}{R}\right)\left[\cosh\left(\frac{\beta_{ns} z}{R}\right) + \tanh\left(\frac{\beta_{ns}\left(H+\frac{h}{2}\right)}{R}\right)\sinh\left(\frac{\beta_{ns} z}{R}\right)\right]\sum_{k=1}^{K} u_{3k} R_k(\bar{r})\, e^{2i\omega t} r dr \tag{29}$$

By introducing Eq. (26) into relation (29), the following expression for the kinetic energy of the fluid is obtained

$$T_f = -\frac{1}{2}\rho_f \Gamma_1 \omega^2 \sum_{s=1}^{\infty}\sum_{k=1}^{K} A_{ns} B_{ns} {u_{zk}}^2\, e^{2i\omega t} \tag{30}$$

Where A_{ns} and B_{ns} are defined in appendix.

2.4 Solution method

The total energy of the system is sum of the kinetic and potential energies of the plate and fluid plus the work done by external forces. Accordingly, the total energy of the system is

$$\Pi = \left(U_p\right)_{max} - \left(T_f + T_p\right)_{max} - W \tag{31}$$

Where W is the work of external non-conservative forces. It is clear that in free vibrations $W = 0$. The Ritz method requires the total energy of Eq. (31) to attain minimum with respect to unknown coefficients, therefore

$$\frac{\partial \Pi}{\partial u_{ri}} = 0,\ \frac{\partial \Pi}{\partial u_{\theta j}} = 0, \frac{\partial \Pi}{\partial u_{zk}} = 0, \frac{\partial \Pi}{\partial \psi_{rl}} = 0,\ \frac{\partial \Pi}{\partial \psi_{\theta q}} = 0 \tag{32}$$

Which leads to following eigenfrequency equation

$$\left(\left[\acute{K}\right] - \omega^2\left[\acute{M}\right]\right)\{\acute{\Delta}\} = 0 \tag{33}$$

In Eq. (33), $\left[\acute{K}\right]$ and $\left[\acute{M}\right]$ are the square stiffness matrix and the mass matrix of dimensions $Sum[I, J, K, L, Q]$. Moreover, $\{\acute{\Delta}\}$ is the column vector as follow

$$\{\acute{\Delta}\} = \{\{u_{ri}\}\ \ \{u_{\theta j}\}\ \ \{u_{zi}\}\ \ \{\psi_{rl}\}\ \ \{\psi_{\theta q}\}\}^T \tag{34}$$

In which

$$\begin{gathered}\{u_{ri}\} = \{u_{r1}\ \ u_{r2}\ \ \dots\ \ u_{rI}\}^T \\ \{u_{\theta j}\} = \{u_{\theta 1}\ \ u_{\theta 2}\ \ \dots\ \ u_{\theta J}\}^T \\ \{u_{zi}\} = \{u_{z1}\ \ u_{z2}\ \ \dots\ \ u_{zK}\}^T \\ \{\psi_{rl}\} = \{\psi_{r1}\ \ \psi_{r2}\ \ \dots\ \ \psi_{rL}\}^T \\ \{\psi_{\theta q}\} = \{\psi_{\theta 1}\ \ \psi_{\theta 2}\ \ \dots\ \ \psi_{\theta Q}\}^T\end{gathered} \tag{35}$$

A non-trivial solution is obtained by setting the determinant of the coefficient matrix of Eq. (33) equal to zero. Roots of the determinant are the square of the eigenvalues (Eigenfrequencies). Eigenfunctions, i.e., mode shapes, corresponding to the eigenvalues are determined by back-substitution of the eigenvalues, one by one, into Eq. (33).

2.5 Formulation for forced vibration of circular plate

Generally, the force applied on the plate is considered as $F = F(r, \theta, t)$. The work done by this force may be expressed as follow

$$W = \int_0^{2\pi}\int_0^{a} F(r,\theta,t)u_3(r,\theta,t)r\,dr\,d\theta \tag{36}$$

Eq. (36) in terms of non-dimensional parameters is written as

$$W = \int_0^{2\pi}\int_{-1}^{1} F(\bar{r},\bar{\theta},t)u_z(\bar{r},\bar{\theta},)\left(\frac{\bar{R}}{2}\right)^2(\bar{r}+\delta)\,d\bar{r}\,d\bar{\theta} \tag{37}$$

Moreover, force $F(\bar{r}, \bar{\theta}, t)$ can be expressed as below

$$F(\bar{r},\bar{\theta},t) = G(\bar{r})\cos n\bar{\theta}\,F(t) \tag{38}$$

Consequently, the eigenfunction expansions for u_r, u_θ, u_z, ψ_r and ψ_θ of the plate for forced vibrations, involves mode shapes of the plate with time dependent amplitude factor $T(t)$. This can be used to derive the related solution (Jafari 2008). According to this method, the displacement domain of the plate exists as follow

$$\begin{gathered}u_r(\bar{r},\bar{\theta},t) = \bar{U}_r(\bar{r})\cos n\bar{\theta}\,T(t) \\ = F_1^a(\bar{r})F_1^b(\bar{r})\sum_{i=1}^{I} u_{ri}R_i(\bar{r})\cos n\bar{\theta}\,T(t)\end{gathered} \tag{39}$$

$$\begin{gathered}u_\theta(\bar{r},\bar{\theta},t) = \bar{U}_\theta(\bar{r})\sin n\bar{\theta}\,T(t) \\ = F_2^a(\bar{r})F_2^b(\bar{r})\sum_{j=1}^{J} u_{\theta j}R_j(\bar{r})\sin n\bar{\theta}\,T(t)\end{gathered} \tag{40}$$

$$\begin{gathered}u_z(\bar{r},\bar{\theta},t) = \bar{U}_z(\bar{r})\cos n\bar{\theta}\,T(t) \\ = F_3^a(\bar{r})F_3^b(\bar{r})\sum_{k=1}^{K} u_{zk}R_k(\bar{r})\cos n\bar{\theta}\,T(t)\end{gathered} \tag{41}$$

$$\begin{gathered}\psi_r(\bar{r},\bar{\theta},t) = \bar{\psi}_r\cos n\bar{\theta}\,T(t) \\ = F_r^a(\bar{r})F_r^b(\bar{r})\sum_{l=1}^{L} \psi_{rl}R_l(\bar{r})\cos n\bar{\theta}\,T(t)\end{gathered} \tag{42}$$

$$\begin{gathered}\psi_\theta(\bar{r},\bar{\theta},t) = \bar{\psi}_\theta\sin n\bar{\theta}\,T(t) \\ = F_\theta^a(\bar{r})F_\theta^b(\bar{r})\sum_{q=1}^{Q} \psi_{\theta q}R_q(\bar{r})\sin n\bar{\theta}\,T(t)\end{gathered} \tag{43}$$

Where $(u_{ri},\ u_{\theta j},\ u_{zk},\ \psi_{rl},\ \psi_{\theta q})$ are the constant coefficients obtained in free vibrations of the plate, and $T(t)$ is an unknown function of time t. The main task is to find a solution for $T(t)$ in the domain of interest.

Inserting Eqs. (38) and (41) into Eq. (36) leads to

$$W = \int_0^{2\pi}\int_{-1}^{1} G(\bar{r})F(t)F_3^a(\bar{r})F_3^b(\bar{r})\sum_{k=1}^{K} u_{zk}R_k(\bar{r})\cos n\bar{\theta}\left(\frac{\bar{R}}{2}\right)^2(\bar{r}+\delta)\,d\bar{r}\,d\bar{\theta} \tag{44}$$

Integrating Eq. (44) with respect to $\bar{\theta}$ yields

$$\begin{gathered}W = \Gamma_1\left(\frac{\bar{R}}{2}\right)^2 F(t)\sum_{k=1}^{K} u_{zk}\int_{-1}^{1} F_3^a(\bar{r})F_3^b(\bar{r})G(\bar{r})(\bar{r} \\ + \delta)R_k(\bar{r})\,d\bar{r}\end{gathered} \tag{45}$$

Applying the Ritz method on the total energy of the system in Eq. (31) results the equations of the system. This gives

$$\left[\acute{M}\right]\{\acute{\Delta}\}\ddot{T}(t) + \left[\acute{K}\right]\{\acute{\Delta}\}T(t) = \{Q\}F(t) \tag{46}$$

In which, $\{\acute{\Delta}\}$ is the column vector of coefficients as below

$$\{\acute{\Delta}\} = \{\{u_{ri}\}\ \ \{u_{\theta j}\}\ \ \{u_{zi}\}\ \ \{\psi_{rl}\}\ \ \{\psi_{\theta q}\}\}^T \tag{47}$$

Moreover, $\{Q\}$ is the column vector that the number of columns is sum of the truncation orders of Chebyshev

polynomials

$$\{\Delta\} = \left\{ \{0\}_I \quad \{0\}_J \quad \left\{ \Gamma_1 \left(\frac{\bar{R}}{2}\right)^2 \sum_{k=1}^{K} \int_{-1}^{1} F_3^a(\bar{r}) F_3^b(\bar{r}) G(\bar{r}) (\bar{r}+\delta) R_k(\bar{r}) d\bar{r} \right\}_K \quad \{0\}_L \quad \{0\}_Q \right\}^T \tag{48}$$

The equations in left side of Eq. (46) are coupled. So, the modal analysis is used to decouple these equations [22]. Using the normalized mode shapes, Eq. (46) becomes

$$[I]\ddot{T}(t) + [I]\omega^2 T(t) = \{\acute{\Delta}\}^T \{Q\} F(t) \tag{49}$$

The solution of Eq. (49) for zero initial conditions is given by

$$T(t) = \frac{\{\acute{\Delta}\}^T \{Q\}}{\omega} \int_0^t F(\tau) \sin \omega(t-\tau)\, d\tau \tag{50}$$

By substituting the time function $T(t)$ into Eqs. (39)-(43), the displacements of the plate are calculated. In this research, the exciting load on the plate in contact with the fluid is assumed to be a harmonic force as follow

$$F(\bar{r}, \bar{\theta}, t) = G(\bar{r}) F(t) = F_0 \sin \Omega t \tag{51}$$

In which, Ω is the constant angular velocity of the force. Inserting Eq. (51) into Eq. (50), time function $T(t)$ is obtained as

$$T(t) = \frac{\{\acute{\Delta}\}^T \{Q\}}{\omega} \frac{\Omega \sin \omega t - \omega \sin \Omega t}{\Omega^2 - \omega^2} \tag{52}$$

3. Results and discussion

In this paper, the forced vibration analysis of moderately thick annular/circular plate made from FG material in contact with fluid is presented. It is assumed that the upper surface of the plate is metal-rich and the lower part of it is ceramic-rich in contact with fluid.

Since there is no available result for the dynamic analysis of annular/circular FGM plate in contact with fluid and under external load, the present approach is validated by considering limit cases. For this purpose, the accuracy of the present formulations is validated by comparing it with the obtained results in (Allahverdizadeh 2008). In mentioned reference, Kantorovich time average technique is employed for forced vibrations of FGM circular plate under harmonic load. However, in its work, the plate was not in contact with fluids. The FG material properties proposed in this work are; $E_m = 70\ GPa$, $E_c = 380\ GPa$, $\rho_m = \rho_c = 3800\ kg/m^3$, $p = 10$ and $\nu = 0.28$. The maximum non-dimensional amplitude at the plate center u_z/h with respect to the first non-dimensional frequency $\omega = a^2\Omega/h\sqrt{12\,\rho_m(1-\nu^2)/E_m}$ -with the ratio of the thickness to radius equal 0.04- is chosen for comparison. Moreover, the amplitude of harmonic force is assumed to be $250N$. Results are shown in Fig. 3. Excellent agreement between these results is observed.

Furthermore, the finite element model of the clamped functionally graded annular plate coupled with fluid is implemented, with $\eta = 0.25$, $\delta = 0.05$, $H = R = 1m$ and $\nu = 0.3$. The non-dimensional deflection $\bar{U}_z = u_z E_m a h/F_0 b$ for the FGM circular plate under harmonic load for various power indexes and thickness/inner radius ratios are compared with finite element results in Table 2. It can be found from Table 2 that the present results are in good agreement with those of finite element model (FEM).

For numerical results, a functionally graded material composed of aluminum (as metal) and alumina (as ceramic) is considered. Young's modulus and density of aluminum and ceramic are $E_m = 70\ GPa$, $\rho_m = 3800\ kg/m^3$ and $E_c = 380\ GPa$, $\rho_c = 4500\ kg/m^3$ respectively. The

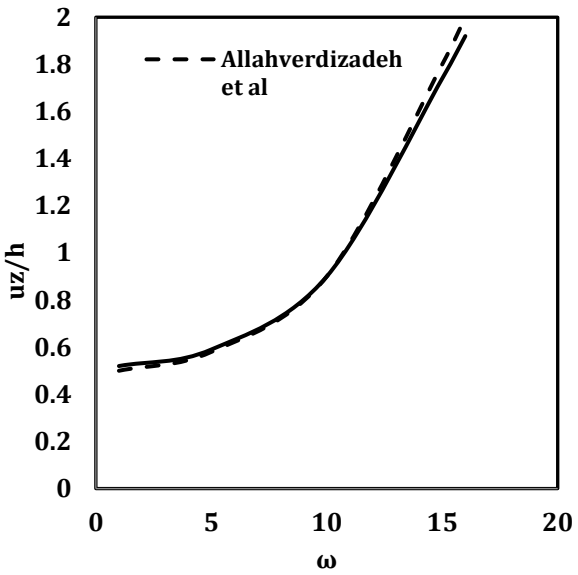

Fig. 3 Comparison between the maximum non-dimensional amplitude at the plate center u_z/h respect to the first non-dimensional frequency ω

Table 2 Comparison between the maximum non-dimensional deflection $\bar{U}_z = u_z E_m a h/F_0 b$ for clamped circular plate in contact with fluid under harmonic load

F_0	h/a	Method	p=0	p=0.5	p=1	p=5	p=10
100	0.05	Present	0.0661	0.0657	0.0738	0.0816	0.0916
		FEM	0.0668	0.0658	0.0740	0.0817	0.0918
	0.1	Present	0.0364	0.0381	0.0442	0.0490	0.0577
		FEM	0.0364	0.0381	0.0443	0.0492	0.0577
	0.2	Present	0.0094	0.0098	0.0113	0.0125	0.0148
		FEM	0.0093	0.0097	0.0112	0.0124	0.0146
200	0.05	Present	0.1301	0.1378	0.1631	0.1807	0.2113
		FEM	0.1306	0.1383	0.1640	0.1819	0.2121
	0.1	Present	0.1306	0.1383	0.1640	0.1819	0.2121
		FEM	0.1301	0.1378	0.1631	0.1807	0.2113
	0.2	Present	0.0856	0.0903	0.1059	0.1174	0.1377
		FEM	0.0856	0.0901	0.1058	0.1173	0.1377
300	0.05	Present	0.3943	0.4268	0.5234	0.5790	0.6688
		FEM	0.3948	0.4284	0.5254	0.5803	0.6688
	0.1	Present	0.2767	0.2969	0.3595	0.3982	0.4622
		FEM	0.2771	0.2980	0.3607	0.3989	0.4623
	0.2	Present	0.1852	0.2074	0.2051	0.2405	0.3258
		FEM	0.1855	0.2079	0.2053	0.2411	0.3261

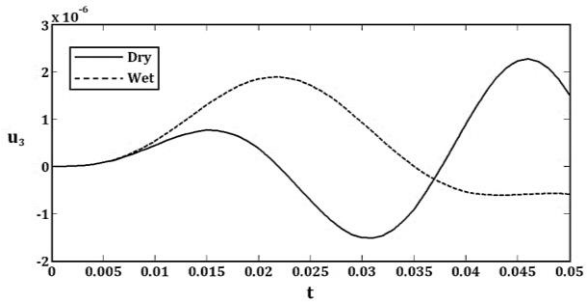

Fig. 4 Dynamic response of the FGM circular plate center under the harmonic load for dry and wet plate

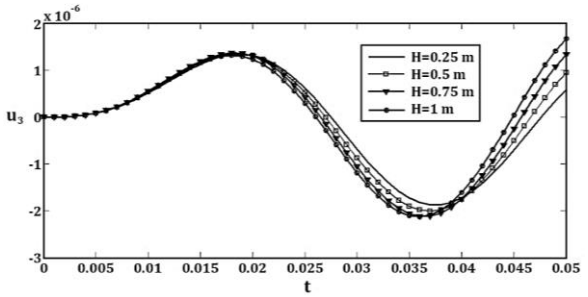

Fig. 5 Dynamic response of the FGM circular plate center under harmonic load for different values of fluid height

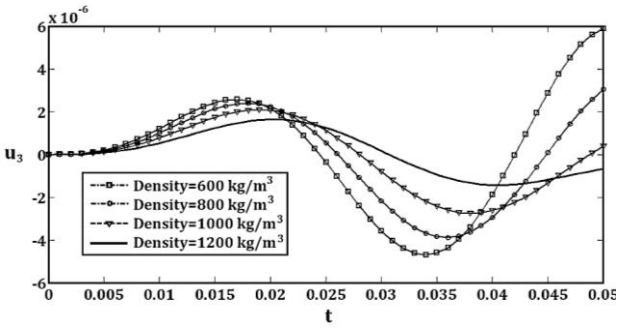

Fig. 6 Dynamic response of the FGM circular plate center under harmonic load for different values of fluid density

Poisson's ratio of the plate is assumed to be constant through the thickness and equal to 0.3. The density of the fluid is assumed to be $1000\ kg/m^3$. Boundary conditions are assumed to be simply-supported on all the plate edges.

In order to study the effects of the fluid presence on the vibrational behavior of the annular FGM plate, the response of the plate center is shown in Fig. 3 for various time t under excited force $F(r,\theta,t) = 100\sin 210t$, for two cases of dry and wet plates. As expected, it can be seen that, the center deflection of the circular FG plate in contact with fluid decreases with the presence of fluid. This is due to the fact that the fluid presence increases the effective system's inertia. It is also observed that the presence of fluid causes delay of the maximum deflection of the plate.

The effects of the variation of the vessel height on the dynamic response of the plate in contact with fluid are illustrated in Fig. 5 for some values of the time t. It is observed that by increasing the fluid height, the dynamic response and the maximum deflection of the plate increase negligibly.

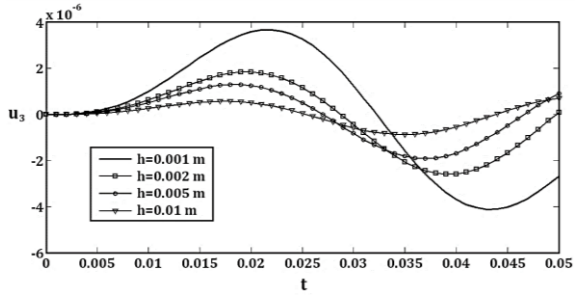

Fig. 7 Dynamic response of the FGM circular plate center under harmonic load for different values of plate thickness

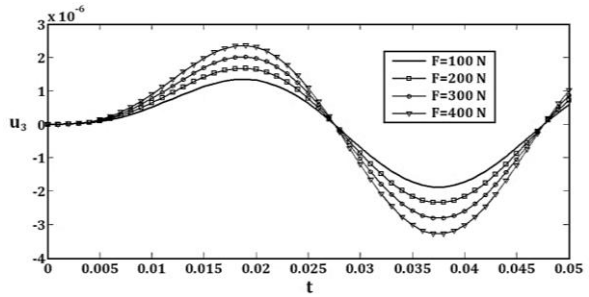

Fig. 8 Dynamic response of the FGM circular plate center under harmonic load for different values of load amplitude

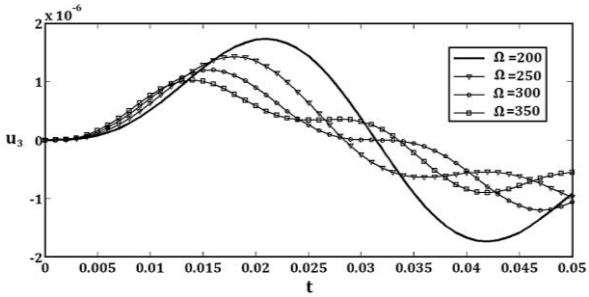

Fig. 9 Dynamic response of the FGM circular plate center under harmonic load for different values of load frequency

To study the effect of fluid density on the dynamic response of FGM circular plate in contact with fluid, Fig. 6 is plotted for different values of time t under harmonic load $f(r,\theta,t) = 100\sin 210t$. It is evident from this figure that, when the plate is oscillated in contact with denser fluids, the maximum deflection of the plate takes lower values. This is due to the fact that the fluid presence causes the increase of the system's inertia. Furthermore, increasing the fluid density leads to a delay in maximum deflection of the plate.

Fig. 7 shows the effect of plate thickness on the dynamic response of the FGM circular plate in contact with fluid for $f(r,\theta,t) = 100\sin 210t$. It is seen that by increasing the plate thickness the maximum deflection of the plate decreases and the amplitude of the plate increases. In other words, the maximum deflection of the plate happens earlier.

The variations of the dynamic response of the circular FGM plate in contact with fluid versus the excited force amplitude are shown in Fig. 8. The results in Fig. 8 indicate that by increasing the force amplitude the deflection amplitude increases but there are no changes in deflection periods.

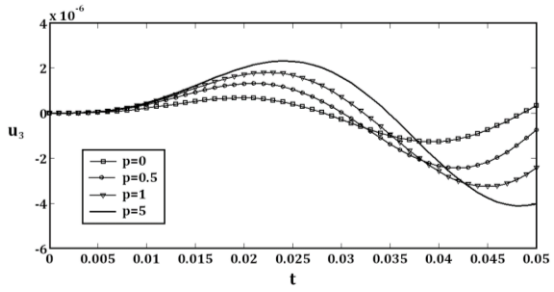

Fig. 10 Dynamic response of the FGM circular plate center under harmonic load for different values of the power index

To study the effect of excited force frequency on the dynamic response of the FGM circular plate in contact with fluid, Fig. 9 is plotted for some values of time t. It is evident from this figure, when the excited force frequency increases, the amplitude of the plate deflection decreases and the maximum deflection happens later in time.

The variations of the dynamic response of the circular FGM plate in contact with fluid versus the power index are shown in Fig. 10. It can be seen that, the center deflection of the circular FG plate in contact with fluid increases with the increase of the material property power index p. This is due to the fact that, by increasing the power index, ceramic percentage in the plate decreases. This leads to a lower stiffness of the plate. Furthermore, the maximum deflection of the plate happens earlier.

4. Conclusions

An analytical solution to the problem of forced vibrations of a FGM circular plate in contact with fluid has been presented. Analysis of the plate was based on First-order Shear Deformation Plate Theory (FSDT). The material properties of the plate, such as modulus of elasticity and mass density were assumed to vary in the thickness direction in accordance with a power law equation. The fluid was assumed to be inviscid and incompressible. The equation governing on the oscillatory behavior of the fluid was obtained by solving Laplace equation and satisfying its boundary conditions. The solution was obtained by a generalized Rayleigh–Ritz method, which incorporates the effect of external force. From the present method, natural frequencies and mode shapes were determined by setting the excited load and the forcing frequency, equal to zero in the expression of the generalized energy functional. The modal superposition approach was used to determine the dynamic response of the plate under harmonic load. The results obtained for forced vibration analysis of the FGM plate are validated by comparing it with appropriate results available in the literature for the case of clamped supported FGM plate. No comparisons with analytical results for forced vibrations of FGM plates in contact with fluid could be made, because of lack of such studies in the literature. Parametric studies have been performed for varying fluid height, power law index, plate thickness and harmonic force amplitude and frequency. From the numerical results, it can be seen that the properties of the vessel and fluid and gradients in material properties play an important role in determining the dynamic response of the FGM plate, in contact with fluid. It should be remarked that the concepts outlined in this study can be extended to all plate boundary conditions. The following conclusions may be drawn from the present analysis:

- The center deflection of the circular FGM plate in contact with fluid decreases with the presence of the fluid and the fluid causes delay of the maximum deflection of the plate.
- By increasing the fluid height, the dynamic response and the maximum deflection of the plate increase negligibly.
- When the plate is oscillated in contact with denser fluids, the maximum deflection of the plate takes lower values. This is due to the fact that the fluid presence causes the increase of the system's inertia. Furthermore, increasing the fluid density leads to a delay in maximum deflection of the plate.
- By increasing the plate thickness the maximum deflection of the plate decreases and the amplitude of the plate increases. Also, the maximum deflection of the plate happens earlier.
- By increasing the force amplitude, the deflection amplitude increases but there are no changes in deflection periods.
- When the excited force frequency increases, the amplitude of the plate deflection decreases and the maximum deflection happens later in time.
- The center deflection of the circular FG plate in contact with fluid increases with the increase of the material property power index p and the maximum deflection of the plate happens earlier.

References

Akgoz, B. and Civalek, O. (2013), "Buckling analysis of linearly tapered micro-columns based on strain gradient elasticity", *Struct. Eng. Mech.*, **48**, 195-205.

Allahverdizadeh, A., Naei, M.H. and Bahrami, M.N. (2008), "Nonlinear free and forced vibration analysis of thin circular functionally graded plates", *J. Sound Vibr.*, **310**(4), 966-984.

Amiri, J.V., Nikkhoo, A., Davoodi, M.R. and Hassanabadi, M.E. (2013), "Vibration analysis of a mindlin elastic plate under a moving mass excitation by eigenfunction expansion method", *Thin-Wall. Struct.*, **62**, 53-64.

Bedroud, M., Nazemnezhad, R., Hosseini-Hashemi, S. and Valixani, M. (2016), "Buckling of FG circular/annular mindlin nanoplates with an internal ring support using nonlocal elasticity", *Appl. Math. Modell.*, **40**, 3185-3210.

Bracewell, R. (1986), *The Fourier Transform and Its Applications*, McGraw-Hill, New York, U.S.A.

Cho, D.S., Kim, B.H., Kim, J.H. and Choi, T.M. (2015), "Frequency response of rectangular plate structures in contact with fluid subjected to harmonic point excitation force", *Thin-Wall. Struct.*, **95**, 276-286.

Civalek, O. (2004), "Application of differential quadrature (DQ) and harmonic differential quadrature (HDQ) for buckling analysis of thin isotropic plates and elastic columns", *Eng. Struct.*, **26**, 171-186.

Civalek, O. (2008), "Discrete singular convolution method and

applications to free vibration analysis of circular and annular plates", *Struct. Eng. Mech.*, **29**, 237-240.
Civalek, O., Korkmaz, A. and Demir, C. (2010), "Discrete singular convolution approach for buckling analysis of rectangular kirchhoff plates subjected to compressive loads on two-opposite edges", *Adv. Eng. Softw.*, **41**, 557-560.
Dong, C.Y. (2008), "Three-dimensional free vibration analysis of functionally graded annular plates using the Chebyshev-ritz method", *Mater. Des.*, **29**(8), 1518-1525.
Fox, L. and Parker, I.B. (1968), *Chebyshev Polynomials in Numerical Analysis*, Oxford University Press, Oxford, U.K.
Haddara, M.R. and Cao, S. (1996), "A study of the dynamic response of submerged rectangular flat plates", *Mar. Struct.*, **9**(10), 913-933.
Hashemi, S.H., Karimi, M. and Taher, H.R.D. (2010), "Vibration analysis of rectangular mindlin plates on elastic foundations and vertically in contact with stationary fluid by the ritz method", *Ocean Eng.*, **37**(2), 174-185.
Hasheminejad, S.M., Khaani, H.A. and Shakeri, R. (2013), "Free vibration and dynamic response of a fluid-coupled double elliptical plate system using mathieu functions", *J. Mech. Sci.*, **75**, 66-79.
Hejripour, F. and Saidi, A.R. (2012), "Nonlinear free vibration analysis of annular sector plates using differential quadrature method", *Proceedings of the Institution of Mechanical Engineers, Part C: Journal of Mechanical Engineering Science* **226**(2), 485-497.
Hosseini-Hashemi, S., Taher, H.R.D., Akhavan, H. and Omidi, M. (2010), "Free vibration of functionally graded rectangular plates using first-order shear deformation plate theory", *Appl. Math. Modell.*, **34**(5), 1276-1291.
Jafari, A.A., Khalili, S.M.R. and Azarafza, R. (2005), "Transient dynamic response of composite circular cylindrical shells under radial impulse load and axial compressive loads", *Thin-Wall. Struct.*, **43**(11), 1763-1786.
Jeong, K.H. (2003), "Free vibration of two identical circular plates coupled with bounded fluid", *J. Sound Vibr.*, **260**(4), 653-670.
Jeong, K.H., Lee, G.M. and Kim, T.W. (2009), "Free vibration analysis of a circular plate partially in contact with a liquid", *J. Sound Vibr.*, **324**(1), 194-208.
Jhung, M.J., Choi, Y.H. and Kim, H.J. (2005), "Natural vibration characteristics of a clamped circular plate in contact with fluid", *Struct. Eng. Mech.*, **21**, 169-184.
Jomehzadeh, E., Saidi, A.R. and Atashipour, S.R. (2009), "An analytical approach for stress analysis of functionally graded annular sector plates", *Mater. Des.*, **30**(9), 3679-3685.
Kerboua, Y., Lakis, A.A., Thomas, M. and Marcouiller, L. (2008), "Vibration analysis of rectangular plates coupled with fluid", *Appl. Math. Modell.*, **32**(12), 2570-2586.
Khdeir, A.A. and Reddy, J.N. (1988), "Dynamic response of antisymmetric angle-ply laminated plates subjected to arbitrary loading", *J. Sound Vibr.*, **126**(3), 437-445.
Khorshidi, K. and Bakhsheshy, A. (2014), "Free natural frequency analysis of an FG composite rectangular plate coupled with fluid using rayleigh-ritz method", *Mech. Adv. Compos. Struct.*, **1**(2), 131-143.
Kwak, M.K. (1997), "Hydroelastic vibration of circular plates", *J. Sound Vibr.*, **201**(3), 293-303.
Kwak, M.K. and Kim, K.C. (1991), "Axisymmetric vibration of circular plates in contact with fluid", *J. Sound Vibr.*, **146**(3), 381-389.
Levy, R. (1996), "Rayleigh-ritz optimal design of orthotropic plates for buckling", *Struct. Eng. Mech.*, **4**, 541-552.
Mehrabadi, S.J., Kargarnovin, M.H. and Najafizadeh, M.M. (2009), "Free vibration analysis of functionally graded coupled circular plate with piezoelectric layers", *J. Mech. Sci. Technol.*, **23**(8), 2008-2021.
Myung, J.J. and Young, H.C. (2003), "Fluid bounding effect on natural frequencies of fluid-coupled circular plates", *KSME Int. J.*, **17**(9), 1297-1315.
Shafiee, A.A., Daneshmand, F., Askari, E. and Mahzoon, M. (2014), "Dynamic behavior of a functionally graded plate resting on Winkler elastic foundation and in contact with fluid", *Struct. Eng. Mech.*, **50**(1), 53-71.
Shen, H.S. (2016), *Functionally Graded Materials. Nonlinear Analysis of Plates and Shells*, CRC Press.
Tahouneh, V. (2014), "Free vibration analysis of bidirectional functionally graded annular plates resting on elastic foundations using differential quadrature method", *Struct. Eng. Mech.*, **52**, 663-686.
Tariverdilo, S., Shahmardani, M., Mirzapour, J. and Shabani, R. (2013) "Asymmetric free vibration of circular plate in contact with incompressible fluid", *Appl. Math. Modell.*, **37**(1), 228-239.
Zhou, D., Au, F.T.K., Cheung, Y.K. and Lo, S.H. (2003), "Three-dimensional vibration analysis of circular and annular plates via the chebyshev-ritz method", *J. Sol. Struct.*, **40**(12), 3089-3105.

PL

Appendix

Coefficients A_{ns} and B_{ns} in Eq. (30) are obtained as below

$$A_{ns}=\frac{\left[\cosh\left(\frac{\beta_{ns}z}{R}\right)+\tanh\left(\frac{\beta_{ns}\left(H+\frac{h}{2}\right)}{R}\right)\sinh\left(\frac{\beta_{ns}z}{R}\right)\right]_{z=-\frac{h}{2}}}{\left(\frac{\beta_{ns}}{R}\right)\left[\sinh\left(\frac{\beta_{ns}\left(\frac{h}{2}\right)}{R}\right)+\tanh\left(\frac{\beta_{ns}\left(H+\frac{h}{2}\right)}{R}\right)\cosh\left(\frac{\beta_{ns}\left(\frac{h}{2}\right)}{R}\right)\right]_{z=-\frac{h}{2}}}$$

or

$$A_{ns}=\frac{\left[\cosh\left(\frac{\beta_{ns}h}{2R}\right)-\tanh\left(\frac{\beta_{ns}\left(H+\frac{h}{2}\right)}{R}\right)\sinh\left(\frac{\beta_{ns}h}{2R}\right)\right]}{\left(\frac{\beta_{ns}}{R}\right)\left[\sinh\left(\frac{\beta_{ns}h}{2R}\right)+\tanh\left(\frac{\beta_{ns}\left(H+\frac{h}{2}\right)}{R}\right)\cosh\left(\frac{\beta_{ns}h}{2R}\right)\right]}$$

And

$$B_{ns}=\int_a^b F_3^a(\bar{r})F_3^b(\bar{r})\frac{\int_a^b F_3^a(\bar{r})F_3^b(\bar{r})\cos^2(k\cos^{-1}\bar{r})\,J_n\left(\frac{\beta_{ns}r}{R}\right)rdr}{\int_a^b r\,{J_n}^2\left(\frac{\beta_{ns}r}{R}\right)dr}J_n\left(\frac{\beta_{ns}r}{R}\right)rdr$$